Radioactivity (RAD)

Anfangerpraktikum Teil III, Physik Department, TUM

Berke Mert
Matr. 03738893

Jedd Page
Matr. 03746102

21. June 2023

Contents

1 Introduction

Radioactivity is omnipresent in the universe and describes any type of energy release due to the decay or state change of atoms. It is also the subject of this lab course. In the following the radioactivity of multiple substances will be studied. In addition to this, it will be shown how this radiation effects the human body.

2 Theoretical foundation

2.1 Radioactivity

There are different reasons for the radioactivity of substances; we can categorize radioactivity by the particles or radiation emitted. In the following the main types of radiation is summarized

1. α**-radiation:** Alpha radiation is characterized by the release of a ^{4}He-ion. The α particles have discrete energy levels, due to the inner configuration of the decomposing atom.

2. $\beta^{\pm}$**-radiation:** Beta radiation is caused by the transition of a nucleon from either a proton to a neutron or vice versa, where plus or minus indicates whether an electron or positron is emitted. The probability of observing β^+-radiation or β^--radiation depends on the the ratio of neutrons to protons in the isotope.

3. **Electron capture:** For electrons orbitals with a probability density within the nuclei of the atom (K, L, ...) it is possible for a proton within the nuclei to capture a bound electron and turn into a neutron. This phenomena is called electron capture. The higher energy electrons then fall into lower energy levels, emitting characteristic radiation.

4. γ**-radiation:** The emitting of photons. Often as a secondary radiation after α-radiation or $\beta^{\pm}$-radiation as an atom may decay into an excited state. [1]

2.2 Activity and Half-life

The decay of nuclei can only be described statistically. We define the activity of a radioactive substance in the following way.

$$A(t) = -\frac{dN(t)}{dt} = \lambda \cdot N(t) \tag{1}$$

Whereby λ is the decay constant, describing the rate of decay. The solution to the differential equation is the law of radioactive decay:

$$A(t) = -\frac{dN(t)}{dt} = \lambda \cdot N_0 \cdot \exp(-\lambda t) = A_0 \cdot \exp(-\lambda t) \tag{2}$$

A further useful quantity is the half-life time. The half-life time of an isotope tells us when half of the unstable nuclei of a given amount of a radioactive substance will have decayed.[1]

$$T_{1/2} = \frac{\ln 2}{\lambda} \tag{3}$$

2.3 Matter interaction

Radiation interacts with matter in different manners, depending on radiation type and the energy level of the radiation. Ionizing radiation is the most important type of radiation, due it's ability to degrade both biological and synthetic matter. Ionizing radiation is by definition radiation that is energetic enough to remove bound electrons from atoms, creating both free electrons and positively charged ions. α- and β-radiation are charged can ionize atoms through the coulomb force. γ radiation relies on a multitude of other processes such as the photo effect, Compton scattering and pair production. Radiation intensity in matter is given by it's exponential dependency on the penetration depth

$$I(d) = I_0 \cdot \exp(-\mu \cdot d) \tag{4}$$

with the absorption coefficient μ [1]

3 Experimental procedure

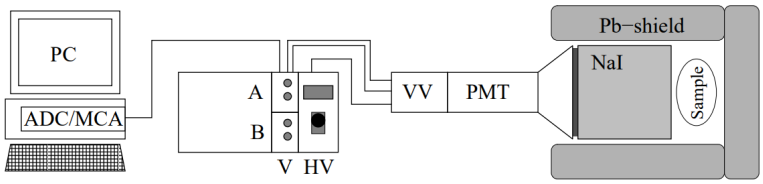

Figure 1: Schematic representation of the experimental setup.

The above figure shows the radiation experiment's setup. Of most importance are the photo-multiplier-tube (PMT), the sodium iodide scintillator, the signal amplification system and the computer system. Furthermore lead blocks are placed around the sample to reduce background noise from external sources. The radiation from the sample interacts with the scintillator, which 'counts' radiation particles through the emission of photons. These photons are absorbed by the photo cathode in the PMT, releasing electrons via the photoeffect these are in turn multiplied through acceleration over dynodes. Where after the PMT outputs an analog signal. This signal is further amplified, before finally being digitised into 1024 Channels. The channels are proportional to the energy of the original radiation and can such be used to analyse the energy spectrum of a sample's radiation. Table 1 gives an overview of the measurements carried out. [1]

measurement	**time**
calibration (Na, Co, Cs)	60s
background (with and without lead)	10min
K2CO3	10min
chernobyl (without lead)	10min
uranium oxide and thorium metal	10min
monozite sand	15min
cosmic radiation	2h

Table 1: Overview of measurements carried out.

4 Evaluation & results

4.1 Energy calibration

Measurements with the experimental setup allow the measurement of the counts in each channel. A relation between the channel number and the energy of the γ-radiation can be derived in the so called energy calibration.
For this purpose, the spectra of calibration sources—^{22}Na, ^{60}Co and ^{137}Cs—with known γ-lines are measured, then the dominant peaks in the spectra are assigned the corresponding energy of the released γ-ray, see figure 2.

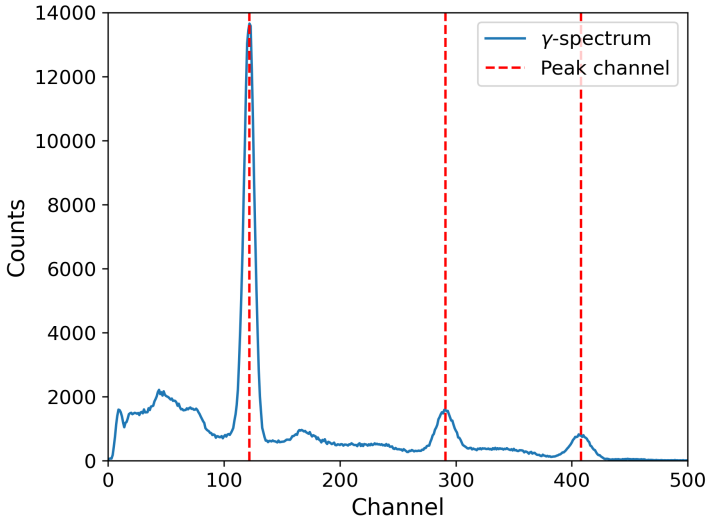

Figure 2: γ-spectrum of ^{22}Na. The channel numbers were determined graphically.

Figure 3 shows the results of the energy calibration with a fit with the function of the form,

$$f(n) = (4.576 \pm 0.047)\,\text{keV} \cdot n + (-61.552 \pm 15.620)\,\text{keV},$$

where n is the channel number and the function output is the energy in keV. From this point on, the energy calibration is used for further experimental evaluation.

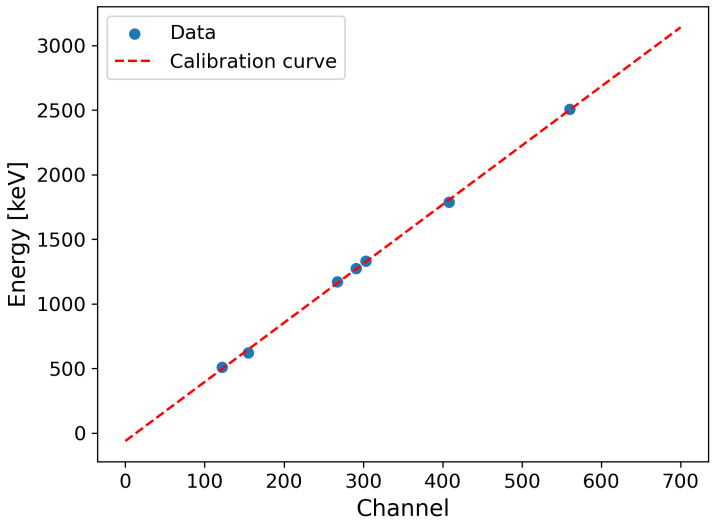

Figure 3: Energy calibration results. The fit results in a linear relation between channel number and energy.

Now, the additional yearly radiation exposure for a person—height $h = 1.80\,\mathrm{m}$, width $w = 0.5\,\mathrm{m}$ and mass $m = 75\,\mathrm{kg}$—is calculated, assuming if the person were to stand $r = 1\,\mathrm{m}$ away from a ^{137}Cs source for his whole life from year 20 up to year 80.
First, the activity of the ^{137}Cs today has to be calculated according to equations (2) and (3). The activity in the year 1992 was at $A_0 = 333\,\mathrm{kBq}$ and the half life time is $T_{1/2} = 30.2\,\mathrm{a}$, therefore the activity this year is $A_0 := 163.47\,\mathrm{kBq}$.
The solid angle the person inhibits equals $\Omega = \frac{h \cdot w}{r^2} = 0.9$, where we assumed the person is a rectangle in the front-view.
The yearly absorbed energy can then be determined as follows,

$$E_{abs} = \frac{E_\gamma^{^{137}\mathrm{Cs}}}{60} \cdot \frac{\Omega}{2\pi} \cdot \int_0^{60} A(t)dt \approx 0.28\ \mathrm{mJ},$$

with which the relation

$$D = \frac{E_{abs}}{m} \tag{5}$$

can be used to determine the yearly absorbed dose, where $D = 0.35\,\mathrm{mSv}$ is obtained.

4.2 Background radiation measurements

The background spectrum with and without a lead shield can be found in figure 4. The shape of the γ-spectra are similar, but number of counts are as expected lower for a detector with a lead shield, $N_{\text{without Pb}} = 114731$ and $N_{\text{with Pb}} = 61437$.
For the following evaluation, the background is always subtracted from the measured γ-spectrum, with an appropriate weight factor—determined by the measurement times of background and measurement sample,

$$N_{corr} = N_{raw} - \alpha \cdot N_{background}.$$

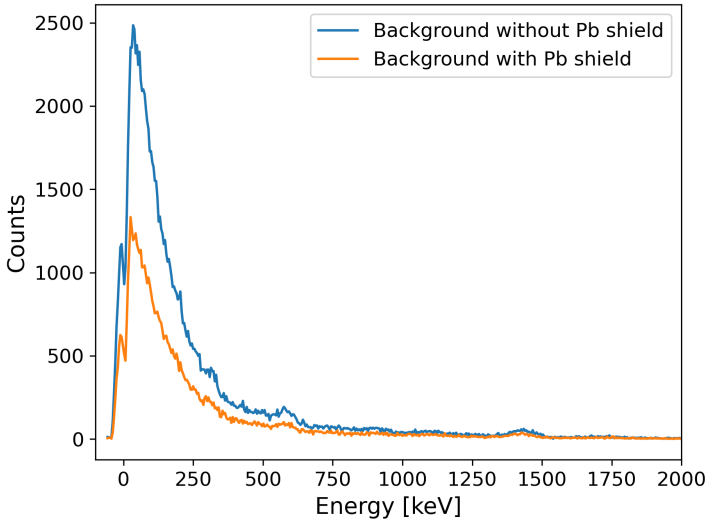

Figure 4: γ-spectrum of background with/without lead shield.

To conclude the discussion of the background spectra, the yearly radiation exposure of the background is determined. First, its assumed that all detected γ-events are verified, and that all low-energy photons with mean energy of 100 keV are absorbed by a human. With the weight of the cylindrical NaI crystal, $m = \rho V \approx 1.29\,\mathrm{kg}$, the yearly absorbed dose can be determined, $D = 74.9\,\mu\mathrm{Sv}$.

4.3 Potassium carbonate sample

Figure 5 shows the "corrected"—meaning free of background—K_2CO_3 spectrum. The measured peak is found by fitting a Gaussian Distribution,

$$G(E) = A \cdot \exp\left(-\frac{(E - E_{mean})^2}{2\sigma^2}\right), \tag{6}$$

which outputs the mean energy of the measured peak, E_{mean}.

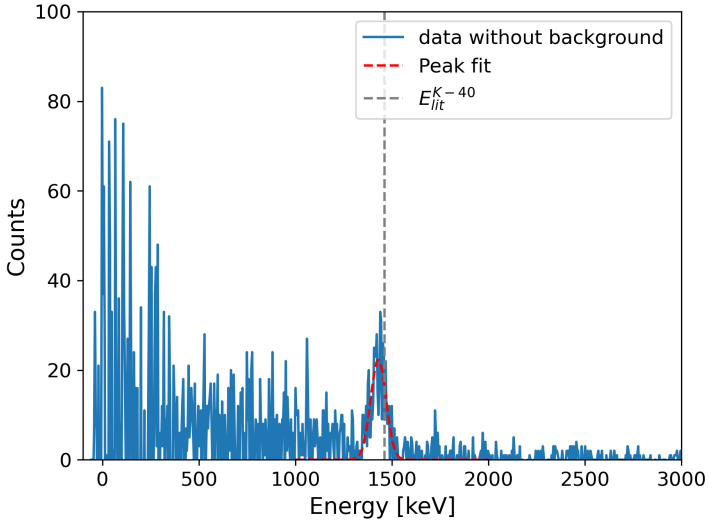

Figure 5: γ-spectrum of K_2CO_3 with literature K-40-γ line and Gauss fit of the measured peak.

In this case, the fit results in $E_{mean} = (1430 \pm 7)\,\text{keV}$, which is not in uncertainty range of the literature value of K-40 capture energy, $E_{lit}^{K-40} = 1461\,\text{keV}$. This is most-likely the consequence of an inaccurate energy calibration, because in reality the relation between energy and channel number is not linear and just a approximation.
After the ten minutes measurement $N = 1424 \pm 38$ K-40 events were registered. The total number of events is determined by summing over the counts of the K-40 peak and the uncertainty with the statistical uncertainty $\sqrt{N}$.
Next step is to determine the activity of the K-40 in the potassium carbonate sample, where we first calculate the number of K_2CO_3. The sample has the mass $m_{sample} = (0.10 \pm 0.01)\,\text{kg}$, where the atoms Potassium, carbon and oxygen have the atomic mass numbers 39, 12 and 16, respectively. The number of K_2CO_3 in the sample is therefore,

$$N = \frac{m_{sample}}{(2M_K + M_C + 3M_O) \cdot C} \approx (4.4 \pm 0.4) \cdot 10^{23},$$

where $C = 1.6605 \cdot 10^{-27} \frac{kg}{amu}$. Because there is only two Potassium atoms in the K_2CO_3 compound, and 0.01% of the atoms in Potassium are radioactive, the number of radioactive K-40 in the sample is $N_{K-40} = (8.7 \pm 0.9) \cdot 10^{19}$. With equation (2) and the half life time of K-40, the activity can be determined, $A = (1.50 \pm 0.15)\,\text{kBq}$, which means the number of detected K-40 events—with a detection probability of 20%—is $N_{theoretical} = (1.8 \pm 0.18) \cdot 10^5$, which is 100 times smaller than the measurement. The sample can emit radiation in every direction, but the solid angle the detector inhibits is small, which is why not every K-40 event can not be detected.

4.4 Chernobyl sample

Figure 6 shows the γ-spectrum of the Chernobyl sample found in Bavaria in the year 1986. The same procedure as in chapter 4.3 to produce this figure and find the mean value of the peaks, which are $E_1^{mean} = (643 \pm 1)\,\text{keV}$ and $E_2^{mean} = (1437 \pm 21)\,\text{keV}$. Comparing the results to the literature values, $E_1^{lit} = 662\,\text{keV}$ and $E_2^{lit} = (1461 \pm 1)\,\text{keV}$ shows, that the measured results are slightly of the literature values, which can be again explained by the inaccurate energy calibration.

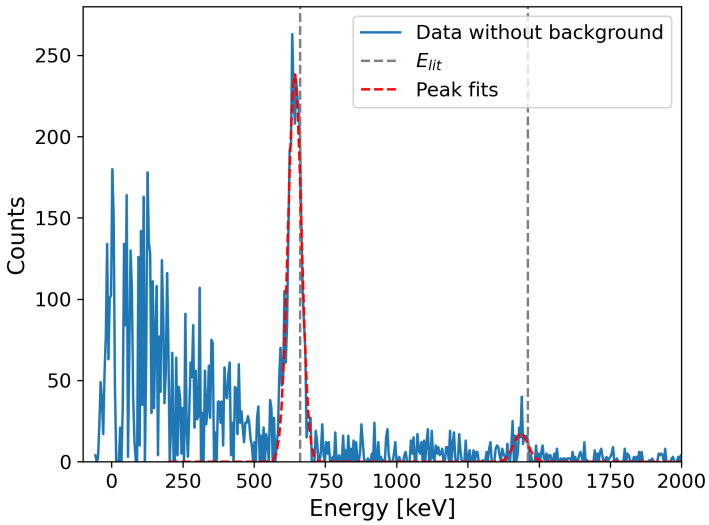

Figure 6: γ-spectrum of the Chernobyl sample with literature K-40 and ^{137}Cs γ-lines and Gauss fit of the measured peaks.

Hypothetically, what would be the radiation exposure of the sample if it were to be eaten? Assuming the sample stays in the human body for one week, all γ-quanta are absorbed by the body, and the energy is normally distributed, the total absorbed energy is determined by,

$$E = N_1 \cdot E_1^\gamma + N_2 \cdot E_2^\gamma \approx 11.12\,\mu\text{eV},$$

with which the absorbed dose of a 80 kg person can be determined to be $D = 140.26\,\text{nSv}$. This means, the sample is not dangerous enough to cause any harm to a human, since the side effect of radiation exposure statistically happen at above 0.01 Sv.

4.5 Uranium and thorium metal

The measured spectra for Uranium oxide and Thorium metal can be seen in figure 7. The characteristic peaks can be clearly identified. The data was obtained by removing the background radiation from the raw data. Vertical lines show the location of the determined peaks. The results can be found in table alongside a comparison to literature values.

Channel	Isotope	E [keV]	E_{lit} [keV]
23	Ur-238	43.7 ± 15.7	50
45	Ra-226	144.4 ± 15.8	186
175	Pa-234	739.3 ± 17.7	767
227	Pa-234	977.2 ± 18.9	1001

Table 2: Results of the uranium oxide sample.

In table 2 the results for uranium oxide are shown. We can see the values of the uranium oxide measurement are in within the uncertainty of most found peaks. The measurement for thorium metal, shown in

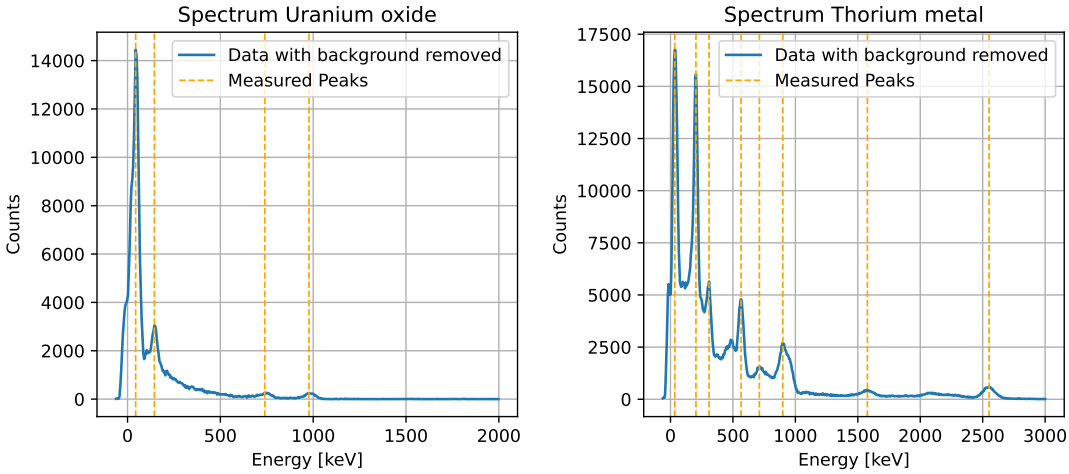

Figure 7: Diagrams showing the measured data for the Uranium oxide and the Thorium metal samples. The vertical lines show the determined characteristic energies.

Isotope	E_{lit}	$E_{thorium}$	$E_{monazite}$
U-238	50	35 ± 16	25 ± 16
Ra-224	241	204 ± 16	204 ± 16
Ac-228	339	309 ± 16	305 ± 16
Tl-208	583	565 ± 17	565 ± 17
Bi-212	727	712 ± 18	716 ± 18
Ac-228	911	899 ± 18	895 ± 18
		1577 ± 23	1572 ± 23
Tl-208	2615	2551 ± 31	2556 ± 31

Table 3: Results of thorium metal and monazite sand compared to literature values.

table 3, produces similar results. The origin of the peaks at circa 1600kEV and 2100keV is explained in 5 and are not found in the thorium series. [1]

4.6 Monazite Sand

In the following section the results of the measurement of a monazite sand sample are presented and discussed. Using the characteristic peaks and comparing them with the known spectra of radioactive isotopes it is possible to determine which elements are found in a sample. Looking at the graph of the monazite sand 8, it is obviously almost indistinguishable to the graph of the thorium sample. We compare the results to the literature values in table 3. Monazite sand contains a large amount of thorium and industrially refined for the pure element.

4.7 Cosmic Radiation

Measuring cosmic radiation, we can determine how much radiation a human absorbs naturally through cosmic radiation. The relatively low intensity of cosmic radiation requires long measurement period in order to obtain accurate measurements.To this end, the detector is placed facing upwards and data is collected for

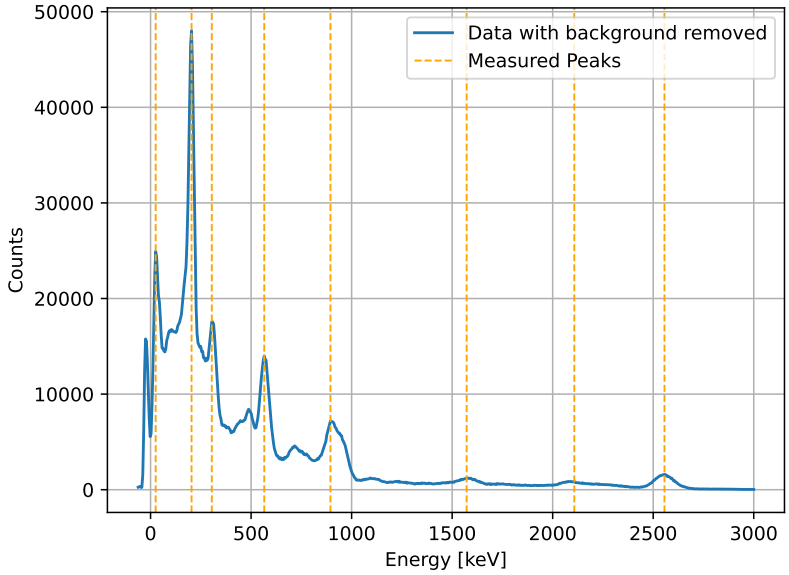

Figure 8: Measurement results of the monazite sand sample. Vertical lines indicate location of characteristic peaks.

two hours. Due to the high energy level of cosmic radiation the detector has to be recalibrated, in order to measure higher energy signals. This is done by lowering the signal amplification so that channels correspond to lower energy levels. We then do a calibration measurement with ^{60}Co, using the characteristic energies of 1173keV, 1333keV and 2506keV. The measured counts and the determined peaks can be seen in 9. The data can then be fitted to a linear function with the form

$$E(n) = a \cdot n + b \tag{7}$$

The fit parameters $a = 49.2 \pm 0.4$keV and $b = 49.2 \pm 0.4$keV are found. **??** The channels are divided into 100 channel zones and the energy level is averaged out in these zones. We then sum over the counts in each of the zones, in doing so we can calculate the energy of the zones. The results are tabulated in 4.

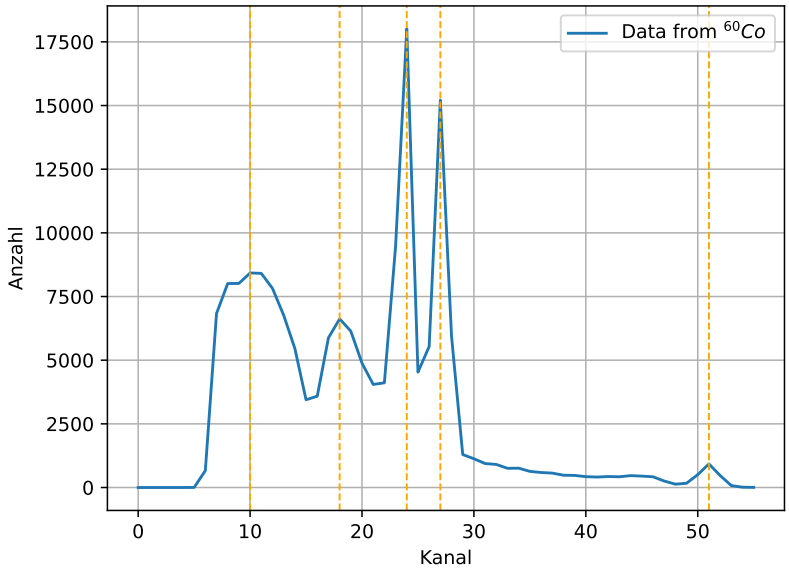

Figure 9: Calibration Data using ^{60}Co, with vertical lines showing found peaks.

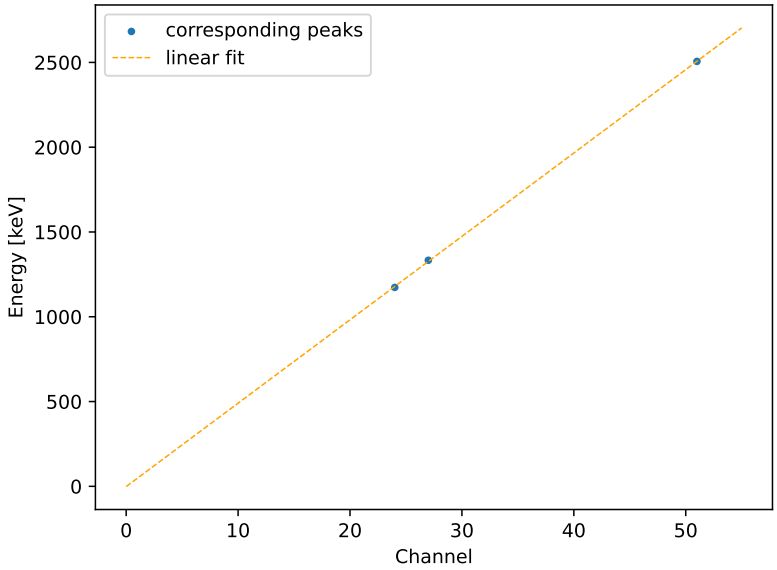

Figure 10: Calibration line with data points.

Channels n	Counts N	Energy EMeV
100 - 199	1669	12310
200 - 299	1243	15281
300 - 399	1086	18692
400 - 499	1032	22838
500 - 599	1059	28644
600 - 699	1361	43505
700 - 799	1143	42158
800 - 899	583	24370
900 - 999	274	12801
Sum	9450	220599

Table 4: Results of the measured cosmic radiation

We see the detector, weighing in at 1.29kg absorbs a total of 22.1GeV in two hours. By roughly approximating one Kilogram of detector material to one Kilogram of human flesh, we can use equation 5 to estimate the amount of cosmic radiation absorbed by a human per year. We find the yearly absorbed dose of a human to be 0.12Sv which in comparison to the literature value of 0.3Sv is a good result considering the simplifications and approximations made.

5 Short questions

1. **How is the unit keV defined? Convert the energy of a cosmic particle ($4 \cdot 10^{12}$ GeV) into Joules. Compare this energy with energies around you.**
   A keV is equivalent to the kinetic energy of an electron which propagates at approximately 6.25% the speed of light, it is a unit used in atomic physics, $1\,\mathrm{eV} = 1.60 \cdot 10^{-19}$ eV. Therefor, the energy of a cosmic particle with $4 \cdot 10^{12}$ GeV is equal to 640.87 J, or for example the energy of a ball with a mass of 1 kg hitting the ground from a height of about 65m.

2. **Why do the peaks in the γ-spectra have finite width? What is meant by FHWM?**
   The width of the peaks underlie Heisenberg uncertainty principle, $\Delta E \cdot \Delta t \leq \frac{\hbar}{2}$, because the decay time of radioactive material is not constant for single decays. Also, there are systematic time measurement uncertainties, because of the equipment used in the experiment. Because the peaks in the spectra have a finite width it makes sense to define a quantity that describes the width of the peak, the so called Full Width at Half Maximum. It is the region of the peak, whose borders are at half the number of counts of the maximum peak.

3. **Explain, of which peaks the ^{22}Na spectrum consist of and where they come from.**
   In the β^+-decay of ^{22}Na, a Positron is emitted that reacts with an electron and produces two γ-quanta, who propagate in opposite directions. The daughter nucleus is in an excited state, and releases a γ-quanta with the energy 1275 keV when falling back to the ground state. The last line comes from the combined measurement of two γ-quanta.

4. **Why is there a γ-line at 77 keV, in the background measurement with a Pb-shield?**
   Pb is in an excited state state and releases a photon with the characteristic energy 77 keV when falling down to its ground state.

5. **In the instruction manual it is stated that the decay of radioactive material is of statistical nature. The uncertainty of the events is $\Delta N = \sqrt{N}$. What does that mean for high number**

of events?
It means the relative uncertainty of the number of events goes to zero according to,

$$u_{rel}(N) = \frac{\Delta N}{\langle N \rangle} = \frac{1}{\sqrt{N}} \to 0 \text{ (for } N \to \infty).$$

6. **In a freshly cleaned long-lived radioactive specimen such as Ra, the activity initially increases. However, before the decrease becomes noticeable according to the decay law, this activity remains nearly constant for a long time. Can you explain this behavior? Consider the generation of daughter nuclei and their decay.**

   This behavior is explained through the decay of daughter isotopes and their generally longer half-life. The daughter isotopes of a radioactive specimen are as a rule more stable than their parent, as such their half-life is longer. So as a freshly cleaned specimen starts to decay, the longer-lived daughter nuclei bottle neck the decay series. Obviously they also contribute to the activity of the sample and as such the activity of a freshly cleaned sample first increases to a plateau, on which it stays for a period of time, before starting to fall according to the law of decay. [2]

7. **How can α-, β- and $\gamma-$radiation be shielded? What about cosmic radiation?**
   For α-radiation, only a sheet of paper suffices. For $\beta-$radiation a couple of millimetres of aluminium is needed. For γ-radiation a couple of centimetres to metres of lead is needed. Cosmic radiation is mostly shielded by the earths magnetic field and is practically very difficult to artificially shield.

8. **"Why do we observe lines at** 2615keV**,** 2104keV**, and** 1593keV **in the thorium decay chain?"**
   ^{208}Th is a part of the thorium decay chain and emits a characteristic γ-quant of 2615keV. This energy is well above the mass of two electrons, with $m_e = 511\text{keV/c}^2$. Which means pair production is possible. After a period of time the produced electron-positron pair annihilates and emits two photons with 511keV each. These photons aren't necessarily detected, causing escape effects. If one Photon escapes without being measured, a so called single escape event, we measure 2104keV. In a double escape event, we measure 1593keV. [3]

9. **How does the measurement with measurement of a γ-event work? Explain it step-by-step from the γ-quantum hitting to showing an event on the software.**
   First, a γ-quantum hits the NaI crystal and interacts with the NaI atoms, so that electrons are released from the crystal structure. The embedded Thalium is then excited by the electrons, which release a flash of light when falling back to its ground state. This ray of light is multiplied by the mirrors in the Photomultiplier and then cast into channels in the detector, which each can be assigned an energy. If the ray of light is produced via the Photoeffect, the whole energy can be detected. In case of the Compton-Effect only a part of the energy can be measured.

6 Error analysis

6.1 Weighted arithmetic mean

To find the mean of multiple values, that have different uncertainties, the weighted arithmetic mean

$$\frac{\sum_{i=1}^{n} w_i \cdot x_i}{\sum_{i=1}^{n} w_i} \tag{8}$$

was used, where w_i are the weights of the different data elements and are given by

$$w_i = \frac{1}{u^2(x_i)}. \tag{9}$$

$u(x_i)$ describe the errors of the different values. To find the uncertainty of the weighted mean, the inner and outer uncertainties are compared. The inner uncertainty is given by

$$u_{int}(\bar{x}) = \sqrt{\frac{1}{\sum_{i=1}^{n} w_i}} \tag{10}$$

and the outer uncertainty by

$$u_{ext}(\bar{x}) = \sqrt{\frac{\sum_{i=1}^{n}(w_i \cdot (x_i - \bar{x})^2)}{(n-1) \cdot \sum_{i=1}^{n} w_i}}. \tag{11}$$

Of the two found uncertainties, the bigger one is used [4].

6.2 Gaussian Error Propagation

For calculations using experimental values with uncertainties the Gaussian formula for error propagation

$$u(\bar{g}) = \sqrt{\sum_{i=1}^{N} (\frac{\delta g}{\delta x_i})^2 u^2(\bar{x_i})}, \tag{12}$$

was used [4].

7 Literature

References

[1] Physics department TUM. Radioactivität (RAD). `https://www.ph.tum.de/academics/org/labs/ap/ap3/RAD.pdf`, 2023. last visited 16.6.2023.

[2] M. Basler, P.A. Tipler, R. Dohmen, G. Mosca, C. Heinisch, A. Schleitzer, M. Zillgitt, J. Wagner, and C. Kommer. *Physik: für Wissenschaftler und Ingenieure*. Springer Berlin Heidelberg, 2014.

[3] W. Demtröder. *Experimentalphysik 3: Atome, Moleküle und Festkörper*. Springer-Lehrbuch. Springer Berlin Heidelberg, 2016.

[4] Physics department TUM. Hinweise zur Beurteilung von Messungen, Messergebnissen und Messunsicherheiten (ABW). `https://www.ph.tum.de/academics/org/labs/ap/org/ABW.pdf`, 20xx. last visited 5.5.2021.